Comparison of radiometric quantities measured in water and above water and derived from SeaWiFS imagery in Onslow Bay and Cape Fear River Plume area.

Piotr Kowalczuk

The University of North Carolina at Wilmington Center for Marine Science, 5600 Marvin Moss Lane, Wilmington, NC 28409, USA kowalczukp@uncwil.edu,

Institute of Oceanology, Polish Academy of Sciences, ul. Powstańców Warszawy 55, PL-81-712, Sopot, Poland, piotr@iopan.gda.pl

Michael J. Durako, William J. Cooper,

The University of North Carolina at Wilmington, Center for Marine Science, 5600 Marvin Moss Lane Wilmington, NC 28409, USA durakom@uncwil.edu , cooperw@uncwil.edu

Abstract

Very few measurements of the bio-optical properties of the South Atlantic Bight have been reported. This paper reports on an ongoing study to better understand the bio-optical properties of a portion of the South Atlantic Bight, the Cape Fear River (CFR) plume. The CFR is one of the largest black-water riverine systems on the eastern coast of the United States and it discharges directly into the lower portion of Onslow Bay and the northern extent of Long Bay. The flow is predominantly southward into Long Bay. Therefore, sampling Onslow Bay provides a baseline coastal system relatively un-impacted by the high dissolved organic waters of the Cape Fear River. The data that we report here were obtained from monthly cruises from October 2001 to April 2002 using two Satlantic radiometric systems: 1) MicroPro, developed for measurements of vertical profiles of downwelled irradiance and upwelled radiance, and 2) MicroSAS, designed to measure the spectral reflectance above the water surface. Measurements have been taken in clear oceanic water at the coastal shelf in Onslow Bay (optical Case I waters) and in turbid Cape Fear River plume waters (optical Case II waters), containing high concentrations of colored dissolved organic matter (CDOM). We have sampled under a range of environmental conditions that include calm and rough seas, and, clear and cloudy skies. Remote sensing reflectance has been calculated at four wavelengths 412, 443, 490, and 555 nm, and results from the two instruments have been compared. The spectrally-averaged unbiased percent difference between remote sensing reflectance, derived from these two approaches, is 19.2 %. The largest difference between the two methods is observed at 555 nm (29.3 %) and the least at 490 nm (11.3 %). Radiometric quantities derived during field measurements, e.g. downwelling irradiance, diffuse attenuation coefficient at 490 nm, spectral remote sensing reflectance and spectral values of normalized water leaving radiances, were compared for available estimates from SeaWiFS images. The biggest random mean square root error (RMSE) between field measurements and SeaWiFS estimates of the remote sensing reflectance has been calculated for the 412 nm wavelength (52.9 %) and the least for the 555 nm waveband (26.3%). The RMSE range calculated between field measurements and SeaWiFS estimates, of normalized water leaving radiances, was 52.9 % for 412 and 23.4 % for 555 nm. The RMSE calculated between field measurement and SeaWiFS estimates of K_d490 was 34.3 %.

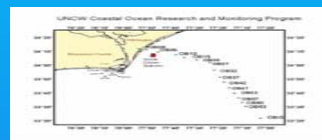

Figure 1. Locations of sample stations in the study area: green dots - Onslow Bay stations, blue dots - Cape Fear River Plume stations, red dots – sub-pixel variability experiment in Onslow Bay.

Experimental setup

The study was performed in Onslow Bay, stations were located along a transect from Masonboro Inlet to the continental shelf break 63 miles south-east from the inlet, and in a grid in the marine portion of the Cape Fear River estuary, at the vicinity of the river mouth (see Figure 1 for the location of the sampling stations).

Data were collected using two sets of radiometers manufactured by Satlanic Inc. - a profiling free-fall radiometer (MicroPro) and an above-water radiometer measuring sky and total reflected radiance (MicroSAS). All data were normalized to incidence irradiance, $E_s(0+,\lambda)$.

Raw sensor data were processed with Prosoft 6.3d processing software, developed and distributed by Satlantic Inc. The raw data were calibrated with calibration coefficients provided by the manufacturer, and then the products were calculated, including spectral values of downwelling irradiance, attenuation coefficient $K_d(\lambda)$, spectral remote sensing reflectance $R_{rs}(\lambda)$ and normalized water leaving radiance $L_{nw}(\lambda)$. Data from the MicroSAS instrument were calibrated and processed according to the procedure called S95 described by Hooker *et al*., (2002). Data were sorted according to 50 lowest values of $L_T(865)$, then the mean value of the 50 lowest readings for each waveband of $L_I(\lambda, \phi, \vartheta^1)$, $L_T(\lambda, \phi, \vartheta)$ and $E_s(0+,\lambda)$ were calculated. Sun glint was removed according to the formula:

$$L_w(\lambda) = L_T(\lambda, \phi^1, \vartheta) - \rho(\lambda,\phi)*L_I(\lambda, \phi^1, \vartheta^1) \quad (1),$$

where: $\rho(\lambda,\phi)$ is the Fresnel reflection coefficient, which for the visible spectrum can be estimated as 0.028 (Mobley, 1999). The spectral reflectance was calculated by normalizing the water leaving radiance $L_w(\lambda)$ to incident solar irradiance above the ocean surface $E_s(0+,\lambda)$:

$$R_{rs}(\lambda) = L_w(\lambda)/E_s(0+,\lambda) \quad (2)$$

Figure 2. Schematic of a Profiling radiometer (from Hooker et al., 1999) and photograph of the MicroPRO (Cyril Dempsey, Satlantic).

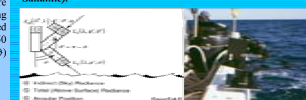

Figure 3. Schematic of a SAS radiometer (from Hooker et al., 1999) and a photograph of the MicroSAS.

Three types of reflectance spectra

1. $R_{rs}(\lambda)$ typical optical Case I waters (Figure 4 - blue lines), characterized by a maximum at 490 nm, elevated values in blue light and close to 0 values in the red - recorded in the Onslow Bay, on the continental shelf, approximately 10 miles or more offshore from Masonboro Inlet

2. $R_{rs}(\lambda)$ typical for optical Case II waters, characterized by maximum in 555 nm, low values in blue light due to CDOM absorption and elevated values in the red due to particle scattering, (Figures 4 and 5 - brown lines) - recorded at Masonboro Inlet and at the Cape Fear River Plume.

3. $R_{rs}(\lambda)$ related to intermediate waters, between the two major optical classifications, usually lower values through the whole spectrum due to weaker scattering and significant decreases in both the blue and red part of the light spectrum, maximum at 490 nm, (Figures 4 and 5 - green lines) - recorded approximately 5-10 miles offshore in Onslow Bay and in the most ocean-side station of the Cape Fear River Plume. In these waters, most of the particles have already precipitated or out of the water column, but CDOM abs

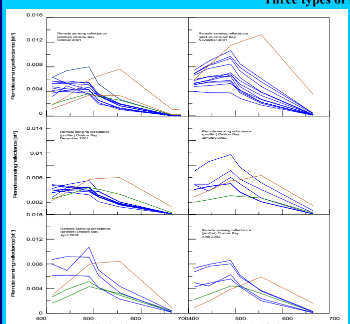

Figure 4. Plots of reflectance spectra measured with the profiling spectroradiometer MicroPro in Onslow Bay from October 2001 till June 2002.

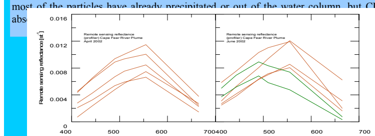

Figure 5. Plots of reflectance spectra measured with the profiling spectroradiometer MicroPro in the Cape Fear River plume April and June 2002.

Comparison of measured radiometric quantities with SeaWiFS imagery data estimates.

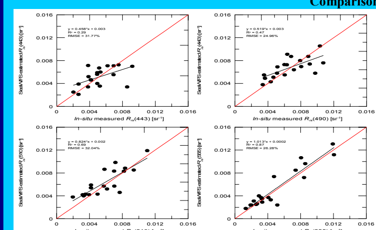

Figure 7. Comparison between remote sensing reflectance measured in-situ and estimated from SeaWiFS imagery data.

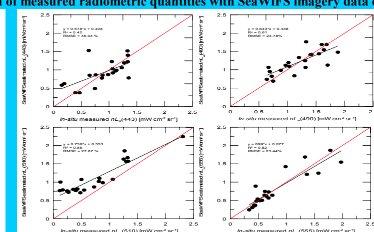

Figure 8. Comparison of normalized water radiances measured in-situ and estimated from SeaWiFS imagery data.

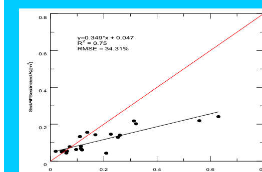

Figure 9. Comparison of downwelling irradiance diffuse attenuation coefficients for λ = 490 nm measured in-situ and estimated from SeaWiFS imagery data.

Comparison of in-water and above-water measurements of spectral remote-sensing reflectance

The unbiased percent difference (UPD) (Hooker et al. 2002) between the two data products X^A and X^B were calculated as:

$$\psi_B^A(\lambda) = \frac{200}{M}\sum_{i=1}^{M}\frac{\left|X_i^A(\lambda) - X_i^B(\lambda)\right|}{X_i^A(\lambda) + X_i^B(\lambda)}$$

where M is the number of measurements and A and B codes identify the method used. In our case *A* would be related to in-water measurements and *B* would be related to above-water measurements. Spectral average of the UPD was calculated by including the summation in equation (3) over the four spectral bands: 412, 443, 490 and 555 nm:

$$\overline{\psi}_B^A = \frac{1}{4}\sum_{j=1}^{4}\psi_B^A(\lambda_j)$$

Table 1. Statistics of calculated differences between in-water and above-water spectral remote-sensing measurements.

Data set	Wavelength	Max. difference %	Min. difference %	Mean difference %	Std. Dev. %	Sample size *N*
Clear sk	412	50.5	0.3	20.7	12.6	24
	443	33.6	0.1	16.3	8.8	
	490	15.7	0.1	11.3	4.9	
	555	37.7	1.3	29.3	11.8	
All data	412	67.7	0.3	32.0	16.4	41
	443	52.0	0.1	28.4	13.7	
	490	41.8	0.1	24.1	11.3	
	555	157.0	1.3	64.5	35.0	

Table 2. Results of the calculated mean UPD between in-water and above-water spectral remote-sensing reflectance measurements for two data sets.

	UPD(412)	*UPD*(443)	*UPD*(490)	*UPD*(555)	Spectrally average UPD
Clear sky conditions *n* = 24	20.7	16.3	11.3	29.3	19.2
All data *n* = 41	32.0	28.4	24.1	64.5	38.0

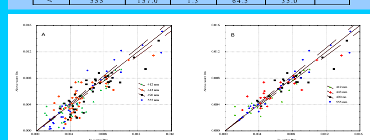

Figure 6. Comparison of in-water and above-water spectral remote sensing reflectance measurements for all data (A) and for clear sky condition (B).

Sub-pixel variability estimation.

- Along ship track above-water measurements of spectral reflectance on Onslow Bay - ship speed 6 knots, sampling resolution - every 7 minutes, measurement duration - 3 minutes, ship heading SW
- Environmental conditions - outgoing tide, less than a 2 ft swell, 1 ft wind waves. During the first two hours of the experiment there were overcast conditions
- 17 spectral measurements, which covered an area of 7 SeaWiFS pixels.

The spatial coverage of the ground-truth measurements on the sub-pixel scale was too small to fully resolve possible patchiness on the signal recorded by the satellite sensor. To get a better overview of the spectral signatures of the water seen by SeaWiFS sensors and to quantify the dispersion in the ground truth and satellite data sets we have calculated descriptive statistics: mean, standard variation and median for the 4 matching wavebands. These results can be seen in the Table 3.

Table 3. Descriptive statistical parameters calculated for in-situ measured and SeaWiFS estimated spectral reflectance.

	In-situ measured $R_{rs}(\lambda)$, *n* =17				SeaWiFS estimated $R_{rs}(\lambda)$, *n* = 7			
	$R_{rs}(412)$	$R_{rs}(443)$	$R_{rs}(490)$	$R_{rs}(555)$	$R_{rs}(412)$	$R_{rs}(443)$	$R_{rs}(490)$	$R_{rs}(555)$
Mean	0.0057	0.0075	0.0100	0.0087	0.0040	0.0069	0.0104	0.0096
Std.Dev	0.0004	0.0004	0.0005	0.0008	0.0009	0.0006	0.0004	0.0008
Median	0.0058	0.0077	0.0101	0.0086	0.0042	0.0073	0.0106	0.0092

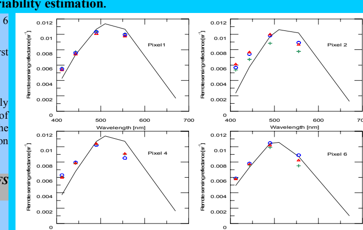

Figure 10. Examples of SeaWiFS estimated remote sensing reflectance spectra (solid lines) and in-situ measured remote sensing reflectance (crosses, triangles and circles) for selected pixels of sub-pixel variability experiment.

Concluding remarks

- Data and results presented here are preliminary in nature.
- Our in-water vs above-water results are more variable than those reported by Hooker et al. 2002 and Zibordi et al., 2002, but we have placed our instruments on a small vessel instead of a fixed platform
- Calculated differences between in water and above water measurements in the range of 10-30% we consider very encouraging.
- The potential of the MicroSAS instrument for ground-truthing SeaWiFS data has been shown in the sub-pixel variability experiment.

References

Hooker, S. B., G. Zibordi, G. Lazin, and S. McLean, 1999. The SeaBOARR-98 Field Campaign. NASA Technical Memorandum 1999-206892, Volume 3; *SeaWiFS Postlaunch Technical Report Series*, S. B. Hooker and E. R. Firestone (eds.), 40 pp.

Hooker S. B., G. Lazin, G. Zibordi, S. McLean, 2002. An evaluation of above- an in-water methods for determining water leaving radiances, *J. Atmos. Ocean Tech*. 19 (4): 486-515.

Mobley C. M., 1999. Estimation of the remote-sensing reflectance from above-surface measurements. *Appl. Opt*. (36):7442-7455.

Zibordi G., S. B. Hooker, J. F., Berthon, D. D'Alimonte, 2002. Autonomous above-water radiance measurements from offshore platform: A field experiment. *J. Atmos. Ocean Tech*. 19 (5): 808-819

Acknowledgment

Research has supported by National Oceanographic & Atmospheric Administration through the Coastal Ocean Research and Monitoring Program (CORMP) conducted at University of North Carolina at Wilmington

Presentation has of this poster has been supported by Office of Naval research through the Visiting Scientist Program, Grant No. N00014-02 -1- 4066